Influence of hygrothermal stress on potential-induced degradation for homojunction and heterojunction crystalline Si photovoltaic modules

Atsushi Masuda[1*†], Chizuko Yamamoto[1], Yukiko Hara[1], Sachiko Jonai[1†], Yasushi Tachibana[2], Takeshi Toyoda[2], Toshiharu Minamikawa[2††], Seira Yamaguchi[3†††], and Keisuke Ohdaira[3]

[1]*Reaserch Center for Photovoltaics, National Institute of Advanced Industrial Science and Technology, Tsukuba, Ibaraki 305-8568, Japan*

[2]*Industrial Research Institute of Ishikawa, Kanazawa, Ishikawa 920-8203, Japan*

[3]*Japan Advanced Institute of Science and Technology, Nomi, Ishikawa 923-1292, Japan*

[*]E-mail: a-masuda@eng.niigata-u.ac.jp

[†]Present address: Graduate School of Science and Technology, Niigata University, Niigata 950-2181, Japan

[††]Present address: Ishikawa Prefectural University, Nonoichi, Ishikawa 921-8836, Japan

[†††]Present address: Graduate School of Engineering, Toyota Technological Institute, Nagoya 468-8511, Japan

Influences of both high-voltage stress and hygrothermal stress were studied for homojunction and heterojunction crystalline Si photovoltaic (PV) modules. In order to separately access the influence of these stresses, these PV modules were subjected to the sequential test with hygrothermal stress and high-voltage stress for various stress durations of each test. It was found that for p-type homojunction crystalline Si PV modules hygrothermal stress applied in advance much enhances potential-induced degradation (PID) by high-voltage stress. High-voltage stress applied in advance also accelerates finger-electrode degradation by hygrothermal stress. It was also clarified that hygrothermal stress for short duration applied in advance much enhances PID by high-voltage stress for n-type heterojunction crystalline Si PV modules. Possible

mechanism for these accelerated degradation phenomena by combined stresses will be presented.

1. Introduction

There have been many reports on dramatic decrease in output power within relatively short period for photovoltaic (PV) plant with high system voltage. These phenomena are usually called potential-induced degradation (PID)[1] and PID is the generic name for such degradation due to potential difference between the cell and grounded frame of the PV module. PID was first found for n-type interdigitated back contact (IBC) crystalline Si PV modules[2] and since 2010 numerous studies were carried out for p-type homojunction crystalline Si PV modules.[3–7] Recently, PID was investigated for almost all kinds of PV modules; for example, not only crystalline Si technologies including n-type homojunction front-emitter type,[8–14] n-type homojunction rear-emitter type,[15] n-type Si heterojunction (SHJ),[11, 16–18] n-type IBC,[19] and p-type passivated emitter and rear cell (PERC),[20] but also thin-film technologies including $Cu(In,Ga)Se_2$,[21,22] CdTe,[23,24] and thin-film Si.[24,25] Especially, Naumann and coworkers[26–29] vigorously studied on the origin of PID for conventional p-type homojunction crystalline Si PV modules and they found that one of the possible origins for the PID is the stacking faults decorated with Na. Such Na originates from not only the cover glass of the PV module but also cell-surface contaminations.[28,30,31]

Various kinds of indoor acceleration test methods for PID were also reported.[32–34] PID test in hygrothermal environment such as 60°C and 85% relative humidity (RH) was often employed following the international standard IEC TS 62804-1.[35] However, in such test conditions, influences of hygrothermal stress and high-voltage stress cannot be separately understood, bringing about obstacle to understanding the mechanism of PID. Since PV modules installed outdoors are exposed to both hygrothermal stress and high-voltage stress, it should be better to clarify the influence of each stress separately and also the effects by combination of both stresses.

On the other hand, our group developed novel indoor PID test method with extremely high acceleration factor.[7,36] In this method Al plate imitating water film on the cover glass in the outdoors was put on the cover glass of PV modules. Conductive rubber sheet was inserted for improving contact between Al plate and cover glass. High-voltage was applied between the grounded Al plate and the shorted interconnectors for both p and n electrodes in the cell. In this test method PID occurs very rapidly for p-type

homojunction crystalline Si PV modules; over 100 times faster than the test regulated by IEC TS 62804-1;[35] for example, maximum power reduces to about 15% of the initial value after the PID test for only 2.5 h at 85°C with −1000 V application.[7] Therefore no change was observed even if adding the humidity in the test environment since influence of water vapor ingress into the PV modules appears after 2000–3000 h in hygrothermal environment at 85°C and 85% RH, which is required for acetic acid generation by hydrolysis reaction between ethylene vinyl acetate (EVA) copolymer encapsulant and water vapor.[37] In this study influences of hygrothermal stress and high-voltage stress were completely separated by conducting sequential test composed of damp heat (DH) test and the above PID test using Al plate in the dry chamber. These tests were carried out for conventional and mostly employed p-type homojunction crystalline Si PV modules and also recently developed high efficiency n-type SHJ PV modules.

2. Experimental methods

The following three kinds of PV cells were employed in this study. The first and the second ones are conventional and commercial p-type front-emitter and Al back-surface field homojunction multicrystalline and monocrystalline Si cells of a size of 156 × 156 mm^2, respectively. The third one is commercial n-type bifacial and rear-emitter monocrystalline SHJ cells of a size of 156 × 156 mm^2. In SHJ cells n^+ and p^+ doped hydrogenated amorphous Si (a-Si:H) layers were prepared on the front and the rear sides of n-type base, respectively, with inserting intrinsic a-Si:H layer between doped a-Si:H layer and n-type base. W doped In_2O_3 films were used for transparent conductive oxide (TCO) layer on both sides of SHJ cells. Those cells were laminated with a tempered cover glass of a thickness of 3.2 mm, two sheets of fast-cure type EVA of a thickness of 450 μm, and a triple layer backsheet composed of polyvinyl fluoride (PVF) film of a thickness of 38 μm, polyethylene terephthalate (PET) base film of a thickness of 250 μm and PVF film of a thickness of 38 μm for p-type homojunction crystalline Si cells and SHJ cells or PET/Al/PET backsheet for SHJ cells. The size of all the PV modules was 180 × 180 mm^2. No Al frame and edge sealant were used for the PV modules employed in this study.

These PV modules were first subjected to DH test in the chamber at 85°C and at 85% RH for imitating hygrothermal stress and second to PID test in the chamber at 85°C and

below 2% RH. DH test durations were 1000–4000 h for p-type homojunction PV modules and 50–700 h for n-type SHJ PV modules. PID test durations and voltage were 5–20 h and −1000 V between shorted interconnector ribbons for both electrodes and the grounded Al plate for p-type homojunction multicrystalline Si PV modules, 0.5–6 h and −1000 V for p-type homojunction monocrystalline Si PV modules, and 3–57 days and −2000 V for n-type SHJ PV modules. p-type homojunction crystalline Si PV modules were also subjected to sequential test composed of DH, PID, and DH tests and to long DH test for 10000 h for comparison. The test was once interrupted after fixed test duration and photo current-voltage (*I*-*V*) characteristics were measured at 25°C using pulsed solar simulator with pulse width of 500 ms, intensity of 100 mW/cm^2 and spectrum of AM1.5. Electroluminescence (EL) images were also observed at 25°C. After photo *I*-*V* and EL measurements the test was resumed with each condition. Leakage current was also measured during PID test.

3. Results and discussion

3.1 Degradation behavior for p-type homojunction crystalline Si PV modules

Figure 1 shows the matrix of EL images for p-type homojunction multicrystalline Si PV modules after PID test following DH test for 1000–4000 h. The PV module without DH test was also subjected to PID test for comparison. It was found that less dark region appears even after PID test for 20 h for the PV module after DH test for 1000 h. On the other hand, dark region appears on the entire cell surface after PID test for 10 h for the PV module after DH test for 2000 h. Such dark region appears faster for the PV module after longer DH test. In the case of the PV modules after DH test for 3000 h and 4000 h no EL image is observed after PID test for 15 h and 5 h, respectively. Figure 2 shows normalized maximum power (P_{max}) as a function of PID test duration for those PV modules after DH tests ranging from 1000 h to 4000 h. Average PV performances obtained by photo *I*-*V* characteristics for these modules before DH test were short-circuit current (I_{sc}) of 8.94 A, open-circuit voltage (V_{oc}) of 0.63 V, fill factor (FF) of 0.73, and efficiency of 17.0%. P_{max} after each DH test is normalized to 1; however P_{max} does not largely change after DH test until 3000 h, and P_{max} after DH test for 4000 h is about 95%

of the initial value, as shown in detail later in Fig. 6. In the case of the PV module without DH test, it is difficult to compare the test results with those for other PV modules after DH test since PID test was continuously carried out until 15 h, then, the recovery from PID during the interruption of measurements cannot occur for the PV modules without DH test. Therefore, test results for the PV modules without DH test are not included in Fig. 2. It was also found from Fig. 2 that normalized P_{max} decreases faster for the PV module with longer DH test before PID test. Such tendency well coincides with that in EL images shown in Fig. 1. Figure 3 shows P_{max} as a function of PID test duration for p-type homojunction monocrystalline Si PV modules after DH tests ranging from 2000 h to 4000 h. Average PV performances obtained by photo *I-V* characteristics for these modules before DH test were I_{sc} of 9.10 A, V_{oc} of 0.63 V, FF of 0.73, and efficiency of 17.2%. Since these monocrystalline Si PV modules are much more susceptible to PID than the multicrystalline Si PV modules shown in Figs. 1 and 2, required PID test duration for drastic reduction is only a few hours and almost no change is observed in the behavior of P_{max} among the PV modules subjected to DH tests prior to PID test. However, similar tendency of P_{max} reduction depending on DH test duration is obtained for both multicrystalline and monocrystalline Si PV modules. These experimental results clearly suggest that PID is easy to occur when hygrothermal stress is given to the PV modules before high-voltage stress is given. P_{max} behavior was also confirmed for monocrystalline Si PV modules with cell and module sizes of 30 × 30 mm^2 and 60 × 60 mm^2, respectively. These small-size cells were obtained by cutting the cell with a size of 156 × 156 mm^2. Although almost similar behaviors were obtained, data scattering is somewhat large (data not shown). This originates not from the data scattering during DH test but from that during PID test since water vapor ingress becomes more uniformly for smaller size modules. Therefore, the data scattering may originate from less uniformity of solar cells, especially less uniformity of anti-reflection coating SiN_x films, which is reported to much affect PID.[38] It was also suggested that one should pay attention to PID test results obtained for small-size cell cut from large-size cell because of influences of the above-mentioned less uniformity in addition to the edge effect, which is also large for small-size cell.

Figures 4 (a) and (b) show leakage current during PID test for the above

multicrystalline and monocrystalline Si PV modules, respectively, without and with DH test ranging from 2000 h to 4000 h. It is found from Figs. 4 (a) and (b) that leakage current drastically increases by one order with DH test for 2000 h. Therefore, acceleration of PID by prior DH test until 2000 h originates from lowering volume resistivity of EVA encapsulant by DH test since electric field applied into antireflection coating SiN_x layer becomes strong with lowering volume resistivity of the encapsulant. The reason why PID is accelerated by prior DH test longer than 3000 h cannot be fully explained only by lowering the volume resistivity of encapsulant since no drastic increase in leakage current with DH test duration is found for both the multicrystalline and monocrystalline Si PV modules subjected to DH test ranging from 2000 h to 4000 h. As shown in Fig. 5, the dark region appears along Ag finger electrodes near busbar electrodes, shown by blue arrows, in the EL image for the multicrystalline Si PV module after DH test for 4000 h. However, after PID test for 6 h following the DH test, the dark region appears near the edge of the cells, as shown by red arrows and no change appears at the dark region generated by DH test shown by blue arrows. This means that origins of the dark regions by DH test and PID test are different. It has been already clarified that the dark region generated by DH test originates from corrosion of the glass layer between Ag finger electrodes and Si emitter layer by acetic acid.[39] On the other hand, as mentioned above, the origin of the dark region generated by PID test is Na incorporation by electric field.[26–29] It is supposed that less electric field is applied around the corroded electrodes and strong electric field concentrates on other regions in comparison with the initial state with all the electrodes in the entire cell without corrosion. This is the possible reason why PID is accelerated for the PV modules subjected to DH test ranging from 2000 h to 4000 h.

Figure 6 shows normalized P_{max} as a function of DH test duration for p-type homojunction multicrystalline Si PV modules. P_{max} was normalized by the initial value before any test. Only DH test was carried out for one PV module. DH test for 1000 h, PID test for 20 h, and again DH test for 3000 h were carried out in this sequence for the other four PV modules. DH and PID test conditions were the same as those shown in Figs. 1 and 2. P_{max} gradually decreases with an increase in DH test duration longer than 4000 h for the PV module subjected to only DH test. P_{max} even after DH test for 10000 h keeps over 70% of its initial value, suggesting that the PV cell has high tolerance against

acetic acid generated by hydrolysis reaction between EVA and water vapor.[40] P_{max} for the other four PV modules keep the initial value after DH test for 1000 h and decreases to about 60% of the initial value after PID test for 20 h. After that P_{max} increases over 80% of the initial value after the following DH test for 1000 h (total 2000 h) and again gradually decreases to about 80 % after the following DH test for 3000 h (total 4000 h). The recovery of P_{max} by DH test for 1000 h just after PID test should originate from heating at 85°C during DH test. Normalized P_{max} values after DH tests for 1000 h (total 2000 h) and 3000 h (total 4000 h) following the PID test correspond to those after only DH test for 6500 h and 8500 h, respectively. Therefore, PID test with high-voltage stress also accelerate the degradation by DH test with hygrothermal stress by about 4500 h. Someone may claim that even if normalized P_{max} values after the DH test following the PID test well coincide with P_{max} values after only DH test, it means that no acceleration of DH test occurs by the prior PID test but such decrease in normalized P_{max} only represents the large drop during PID test. However, such claim is misleading. In the EL images for the PV modules after DH test for 1000 h, 2000 h and 3000 h following the PID test shown in Fig. 6 really indicate that the dark regions appear along finger electrodes near busbar electrodes. These EL images with dark region along finger electrodes are one of the characteristic features of PV modules degraded by DH test as similar EL images are obtained for the PV module subjected to only DH test also shown in Fig. 5 (a). Therefore, it is demonstrated that high-voltage stress really accelerates the degradation by the following hygrothermal stress for p-type homojunction multicrystalline Si PV modules. The reason is not clear so far; however, change in finger electrodes during PID test, for example Na accumulation on finger electrodes,[41] may relate with easy degradation of finger electrodes by a small amount of acetic acid generated by DH test.

3.2 Degradation behavior for n-type SHJ PV modules

With increasing DH test duration P_{max} for SHJ PV modules using PVF/PET/PVF backsheet gradually decreases and about 85% of the initial value after DH test for 700 h. On the other hand, little change in P_{max} was observed for SHJ PV modules using PET/Al/PET backsheet even after DH test for 700 h. PID test was carried out for those SHJ PV modules experienced with DH test.

Figure 7 shows transition of photo *I-V* characteristics for the SHJ PV modules using PVF/PET/PVF backsheet during PID test. PID test durations are 15 days, 21 days, 45 days and 54 days for the SHJ PV modules subjected to DH test for 500 h, 200 h and 50 h, and that without DH test, respectively. For the SHJ PV module without DH test I_{sc} decreases in the first stage of the PID test until 30 days, then, both I_{sc} and V_{oc} decrease in the second stage of the PID, as previously reported by our group.[18] On the other hand, for the SHJ PV modules after DH test, as DH test duration increases, less large degradation is observed after DH test; however, not only PID in the first stage but also PID in the second stage rapidly occurs. As a result, a decrease in I_{sc} in the first stage is hard to be observed due to the merging into the degradation in the second stage. These results suggest that hygrothermal stress accelerates PID phenomena in the SHJ PV modules. Figures 8 and 9 show normalized photo *I-V* parameters, I_{sc}, V_{oc}, FF and P_{max}, as a function of PID test duration, for the SHJ PV modules using PVF/PET/PVF and PET/Al/PET backsheets, respectively. These parameters are normalized by each initial value before DH test. It is found from both Figs. 8 and 9 that decrease in both I_{sc} and V_{oc} appears much earlier and progresses much faster as DH test duration becomes longer. It was also found that decrease in both I_{sc} and V_{oc} progresses somewhat earlier for the SHJ PV module using PVF/PET/PVF backsheet than that for PET/Al/PET backsheet. In this study since no edge sealant is utilized, the difference in amount of water vapor infiltrating into the PV module between the SHJ PV modules using PVF/PET/PVF and PET/Al/PET backsheets is not so large. If edge sealant is utilized, degradation for the SHJ PV modules using PET/Al/PET backsheet may progress more slowly. Increase in FF for the SHJ PV modules using both backsheets may originate from change in the maximum power point due to reduction in I_{sc} or both I_{sc} and V_{oc} in the first or the second PID stage with little change in shunt resistance and series resistance.

The reason why the first stage PID, decrease in I_{sc} due to reduction in TCO, for the SHJ PV modules is accelerated by the DH test prior to PID test is that the following reduction reaction of W-doped In_2O_3 TCO layer is enhanced by the water vapor ingress during DH test. Such reduction reaction was observed by X-ray absorption fine structure spectroscopy and the reduction mechanism was in detail discussd by our previous paper.[18]

$$H_2O + Na \rightarrow NaOH + H, \quad (1)$$

$$In_2O_3 + 6H \rightarrow 2In + 3H_2O. \quad (2)$$

Here, Na may be drifted from the cover glass by high-voltage stress or exist on TCO as surface contamination. The second stage PID is also accelerated by DH test with relatively short duration for only 50–200 h. Such acceleration also originates from lowering of volume resistivity of EVA with DH test duration, as shown in Fig. 10.

4. Conclusions

Both in p-type homojunction conventional crystalline Si PV modules and n-type SHJ PV modules, larger and faster PID occurred in the earlier stage by longer DH test prior to PID test although characteristic features and origins of PID are much different from each other. It was also found that degradation with corrosive Ag finger electrodes by DH test is accelerated by PID test in advance. For SHJ PV modules, not only a decrease in I_{sc} in the first stage but also deceases in both I_{sc} and V_{oc} in the second stage appear earlier with longer DH test duration. PID in the first stage is merged with the PID in the second stage in the case with longer DH test in advance. These experimental results strongly suggest that if PV modules are installed in the tropical zone, strict countermeasure for PID is required.

Acknowledgments

This work was supported by the New Energy and Industrial Technology Development Organization.

References

1) W. Luo, Y. S. Khoo, P. Hacke, V. Naumann, D. Lausch, S. P. Harvey, J. P. Singh, J. Chai, Y. Wang, A. G. Aberle, and S. Ramakrishna, Energy Environ. Sci. **10**, 43 (2017).
2) R. Swanson, M. Cudzinovic, D. DeCeuster, V. Desai, J. Jürgens, N. Kaminar, W. Mulligan, L. Rodrigues-Barbosa, D. Rose, D. Smith, A. Terao, and K. Wilson, Tech. Dig. 15th Int. Photovoltaic Science & Engineering Conf., 2005, p. 410.
3) P. Hacke, M. Kempe, K. Terwilliger, S. Glick, N. Call, S. Johnston, S. Kurtz, I. Bennett, and M. Kloos, Proc. 25th European Photovoltaic Solar Energy Conf. Exhib. / 5th World Conf. Photovoltaic Energy Conversion, 2010, p. 3760.
4) S. Pingel, O. Frank, M. Winkler, S. Daryan, T. Geipel, H. Hoehne, and J. Berghold, Proc. 35th IEEE Photovoltaic Specialists Conf., 2010, p. 2817.
5) J. Berghold, O. Frank, H. Hoehne, S. Pingel, B. Richardson, and M. Winkler, Proc. 25th European Photovoltaic Solar Energy Conf. Exhib. / 5th World Conf. Photovoltaic Energy Conversion, 2010, p. 3753.
6) M. Schütze, M. Junghänel, O. Friedrichs, R. Wichtendahl, M. Scherff, J. Müller, and P. Wawer, Proc. 26th European Photovoltaic Solar Energy Conf. Exhib., 2011, p. 3097.
7) A. Masuda, M. Akitomi, M. Inoue, K. Okuwaki, A. Okugawa, K. Ueno, T. Yamazaki, and K. Hara, Curr. Appl. Phys. **16**, 1659 (2016).
8) K. Hara, S. Jonai, and A. Masuda, Sol. Energy Mater. Sol. Cells **140**, 361 (2015).
9) S. Yamaguchi, A. Masuda, and K. Ohdaira, Appl. Phys. Express **9**, 112301 (2016).
10) S. Bae, W. Oh, K. D. Lee, S. Kim, H. Kim, N. Park, S.-I. Chan, S. Park, Y. Kang, H.-S. Lee, and D. Kim, Energy Sci. Eng. **5**, 30 (2017).
11) K. Hara, K. Ogawa, Y. Okabayashi, H. Matsuzaki, and A. Masuda, Sol. Energy Mater. Sol. Cells **166**, 132 (2017).
12) Y. Komatsu, S. Yamaguchi, A. Masuda, and K. Ohdaira, Microelectron. Reliab. **84**, 127 (2018).
13) S. Yamaguchi, K. Nakamura, A. Masuda, and K. Ohdaira, Jpn. J. Appl. Phys. **57**, 122301 (2018).
14) K. Ohdaira, Y. Komatsu, T. Suzuki, S. Yamaguchi, and A. Masuda, Appl. Phys. Express **12**, 064004 (2019).
15) S. Yamaguchi, A. Masuda, and K. Ohdaira, Sol. Energy Mater. Sol. Cells **151**, 113 (2016).

16) Z. Xiong, T. M. Walsh, and A. G. Aberle, Energy Procedia **8**, 384 (2011).
17) S. Yamaguchi, C. Yamamoto, K. Ohdaira, and A. Masuda, Sol. Energy Mater. Sol. Cells **161**, 439 (2017).
18) S. Yamaguchi, C. Yamamoto, K. Ohdaira, and A. Masuda, Prog. Photovoltaics **26**, 697 (2018).
19) V. Naumann, T. Geppert, S. Großer, D. Wichmann, H.-J. Krokoszinski, M. Werner, and C. Hagendorf, Energy Procedia **55**, 498 (2014).
20) K. Sporleder, V. Naumann, J. Bauer, S. Richter, A. Hähnel, S. Großer, M. Turek, and C. Hagendorf, Phys. Status Solidi RRL **13**, 1900163 (2019).
21) S. Yamaguchi, S. Jonai, K. Hara, H. Komaki, Y. Shimizu-Kamikawa, H. Shibata, S. Niki, Y. Kawakami, and A. Masuda, Jpn. J. Appl. Phys. **54**, 08KC13 (2015).
22) P. Hacke, K. Terwilliger, S. H. Glick, G. Perrin, J. Wohlgemuth, S. Kurtz, K. Showalter, J. Sherwin, E. Schneller, S. Barkaszi, and R. Smith, J. Photon. Energy **5**, 053083 (2015).
23) P. Hacke, S. Spataru, S. Johnston, K. Terwilliger, K. VanSant, M. Kempe, J. Wohlgemuth, S. Kurtz, A. Olsson, and M. Propst, IEEE J. Photovoltaics **6**, 1635 (2016).
24) A. Masuda, Y. Hara, Y. Shiina, S. Okamoto, and T. Okamoto, Jpn. J. Appl. Phys. **58**, SBBF07 (2019).
25) A. Masuda and Y. Hara, Jpn. J. Appl. Phys. **56**, 04CS04 (2017).
26) V. Naumann, D. Lausch, A. Graff, M. Werner, S. Swatek, J. Bauer, A. Hähnel, O. Breitenstein, S. Großer, J. Bagdahn, and C. Hagendorf, Phys. Status Solidi RRL **7**, 315 (2013).
27) V. Naumann, D. Lausch, A. Hähnel, J. Bauer, O. Breitenstein, A. Graff, M. Werner, S. Swatek, S. Großer, J. Bagdahn, and C. Hagendorf, Sol. Energy Mater. Sol. Cells **120**, 383 (2014).
28) V. Naumann, D. Lausch, and C. Hagendorf, Energy Procedia **77**, 397 (2015).
29) V. Naumann, C. Brzuska, M. Werner, S. Großer, and C. Hagendorf, Energy Procedia **92**, 569 (2016).
30) S. Jonai and A. Masuda, AIP Adv. **8**, 115311 (2018).
31) S. Jonai, A. Tanaka, K. Muramatsu, G. Saito, K. Nakamura, A. Ogura, Y. Ohshita, and A. Masuda, Sol. Energy **188**, 1292 (2019).
32) P. Hacke, R. Smith, K. Terwilliger, G. Perrin, B. Sekulic, and S. Kurtz, Prog.

Photovoltaics **22**, 775 (2014).

33) P. Hacke, K. Terwilliger, S. Glick, G. Tamizhmani, S. Tatapudi, C. Stark, S. Koch, T. Weber, J. Berghold, S. Hoffmann, M. Koehl, S. Dietrich, M. Ebert, and G. Mathiak, IEEE J. Photovoltaics **5**, 94 (2015).
34) P. Hacke, K. Terwilliger, R. Smith, S. Glick, J. Pankow, M. Kempe, S. Kurtz, I. Bennett, and M. Kloos, Proc. 37th IEEE Photovoltaic Specialists Conf., 2011, p. 814.
35) IEC TS 62804-1, Ed. 1.0, 2015.
36) K. Hara, H. Ichinose, T. N. Murakami, and A. Masuda, RSC Adv. **4**, 44291 (2014).
37) A. Masuda, N. Uchiyama, and Y. Hara, Jpn. J. Appl. Phys. **54**, 04DR04 (2015).
38) S. Jonai, Y. Tachibana, K. Nakamura, Y. Ishikawa, Y. Uraoka, and A. Masuda, Proc. 46th IEEE Photovoltaic Specialists Conf., 2019, p. 1969.
39) T. Tanahashi, N. Sakamoto, H. Shibata, and A. Masuda, IEEE J. Photovoltaics **8**, 997 (2018).
40) A. Masuda and Y. Hara, Jpn. J. Appl. Phys. **57**, 04FS06 (2018).
41) F. Ohashi, Y. Mizuno, H. Yoshida, H. Kosuga, T. Furuya, R. Fuseya, R. J. Freitas, Y. Hara, A. Masuda, and S. Nonomura, Jpn. J. Appl. Phys. **57**, 08RG05 (2018).

Figure Captions

Fig. 1. (Color online) Matrix of EL images for p-type homojunction multicrystalline Si PV modules after PID test ranging from 0 h to 20 h following DH test ranging from 0 h to 4000 h.

Fig. 2. (Color online) Normalized P_{max} as a function of PID test duration following DH test for various test durations for p-type homojunction multicrystalline Si PV modules. Two or four PV modules were subjected to each test and the average normalized P_{max} values are shown with error bars. Lines serve as visual guides.

Fig. 3. (Color online) Normalized P_{max} as a function of PID test duration following DH test for various test durations for p-type homojunction monocrystalline Si PV modules. One PV module was subjected to each test. Lines serve as visual guides.

Fig. 4. (Color online) Leakage current during PID test for p-type homojunction multicrystalline (a) and monocrystalline (b) Si PV modules. PID test for about 100 h was carried out two times for the multicrystalline Si PV module without DH test shown by blue symbols and that subjected to DH test for 2000 h shown by green symbols. PID test for about 100 h was carried out three times for the multicrystalline Si PV module subjected to DH test for 3000 h shown by orange symbols and that for 4000 h shown by red symbols. PID test for about 80-100 min was carried out for the monocrystalline Si PV module subjected to DH tests for various durations or that without DH test.

Fig. 5. (Color online) EL image for p-type homojunction multicrystalline Si PV module after DH test for 4000 h (a) and for that after PID test for 6 h following DH test for 4000 h. Blue and red arrows show the dark regions appearing by DH and PID tests, respectively.

Fig. 6. (Color online) Normalized P_{max} as a function of DH test duration for p-type homojunction multicrystalline Si PV modules. One PV module was subjected to only DH test for 10000 h and the normalized P_{max} values were shown by open blue symbols. The other four PV modules were subjected to sequential test composed of DH test for 1000 h,

PID test for 20 h, and DH test for 3000 h and the average normalized P_{max} values were shown by closed brown symbols with error bars. Lines serve as visual guides. EL images before and after tests are also shown.

Fig. 7. (Color online) Photo *I-V* characteristics for SHJ PV modules using PVF/PET/PVF backsheet subjected to PID test without DH test (a) and following DH test for 50 h (b), 200 h (c), and 500 h (d). Blue and red arrows approximately show the first and the second stage of PID, respectively.

Fig. 8. (Color online) Normalized I_{sc}, V_{oc}, FF and P_{max} for SHJ PV modules with PVF/PET/PVF backsheet after DH test ranging from 50 h to 700 h or without DH test as a function of PID test durations. All parameters are normalized by each initial value before DH test. Data from two PV modules were shown for each test. Lines serve as visual guides.

Fig. 9. (Color online) Normalized I_{sc}, V_{oc}, FF and P_{max} for SHJ PV modules with PET/Al/PET backsheet after DH test ranging from 50 h to 700 h or without DH test as a function of PID test durations. All parameters are normalized by each initial value before DH test. Data from two PV modules were shown for each test. Lines serve as visual guides.

Fig. 10. (Color online) Leakage current during PID test for SHJ PV modules without prior DH test or subjected to DH test ranging from 50 h to 700 h. PID test for about 80–100 min was carried out.

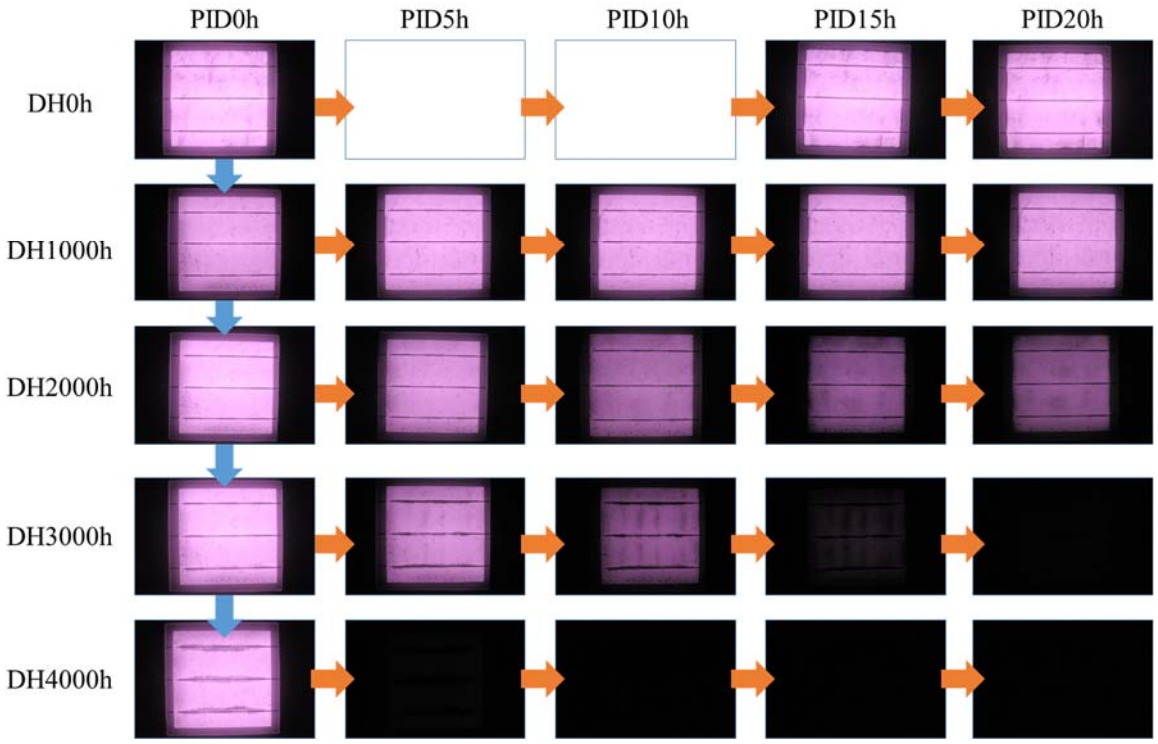

Fig. 1. (Color Online)

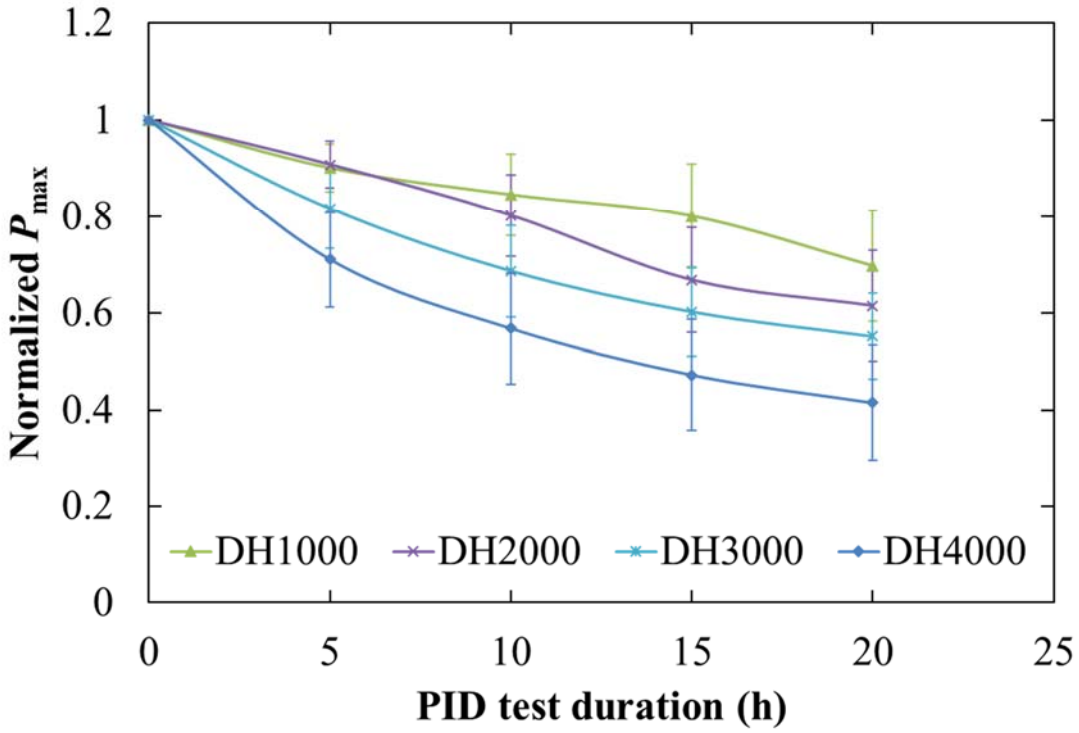

Fig. 2. (Color Online)

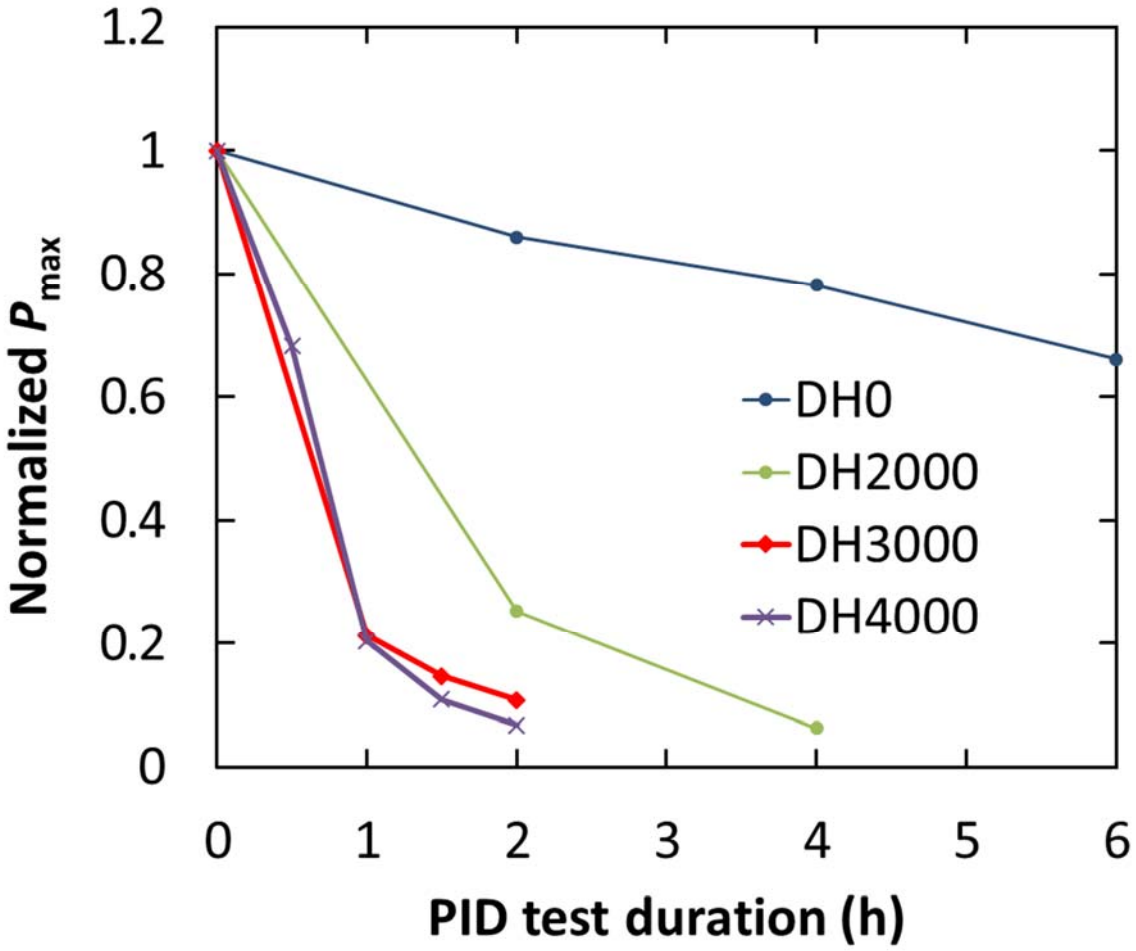

Fig. 3. (Color Online)

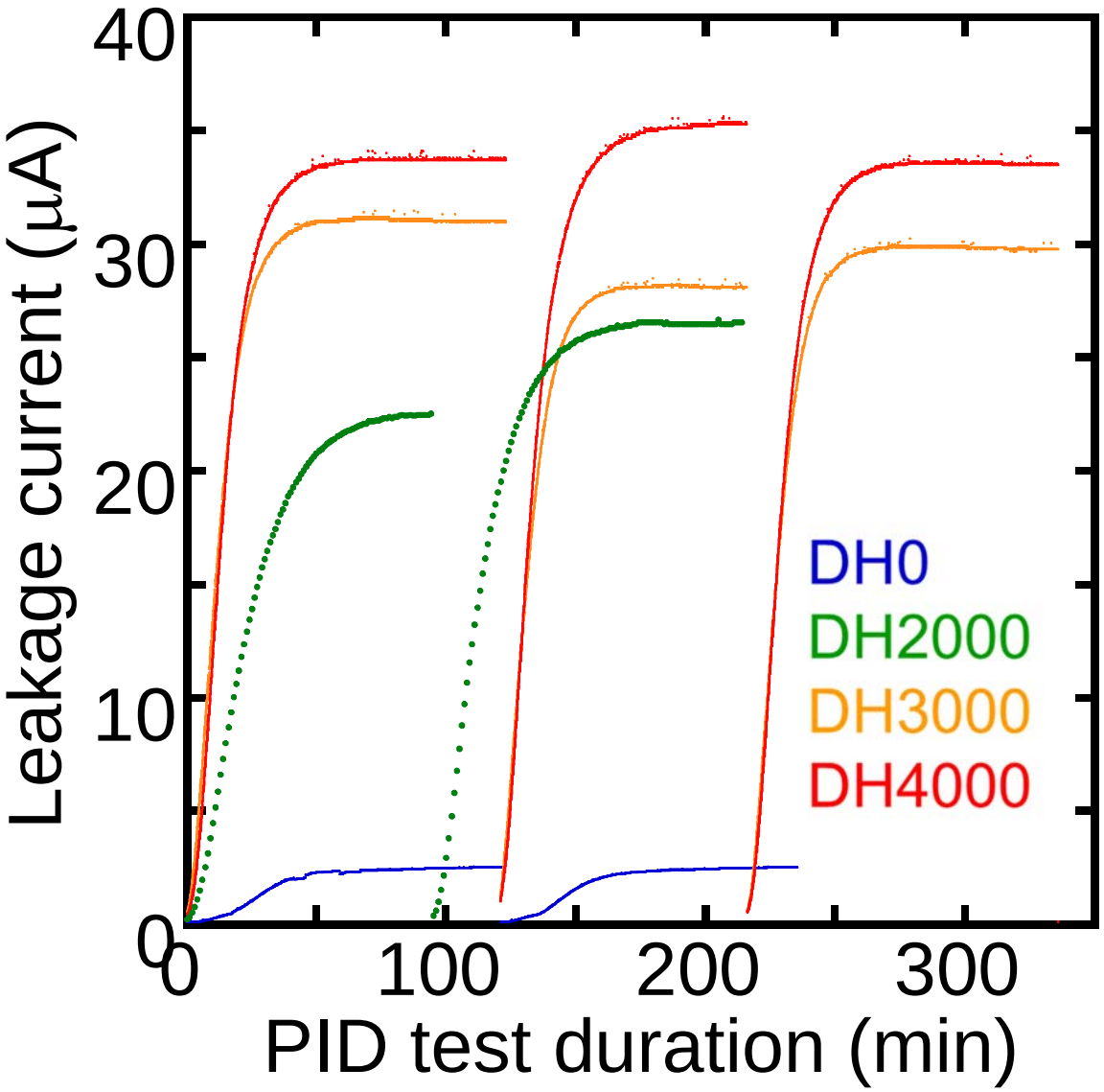

Fig. 4 (a). (Color online)

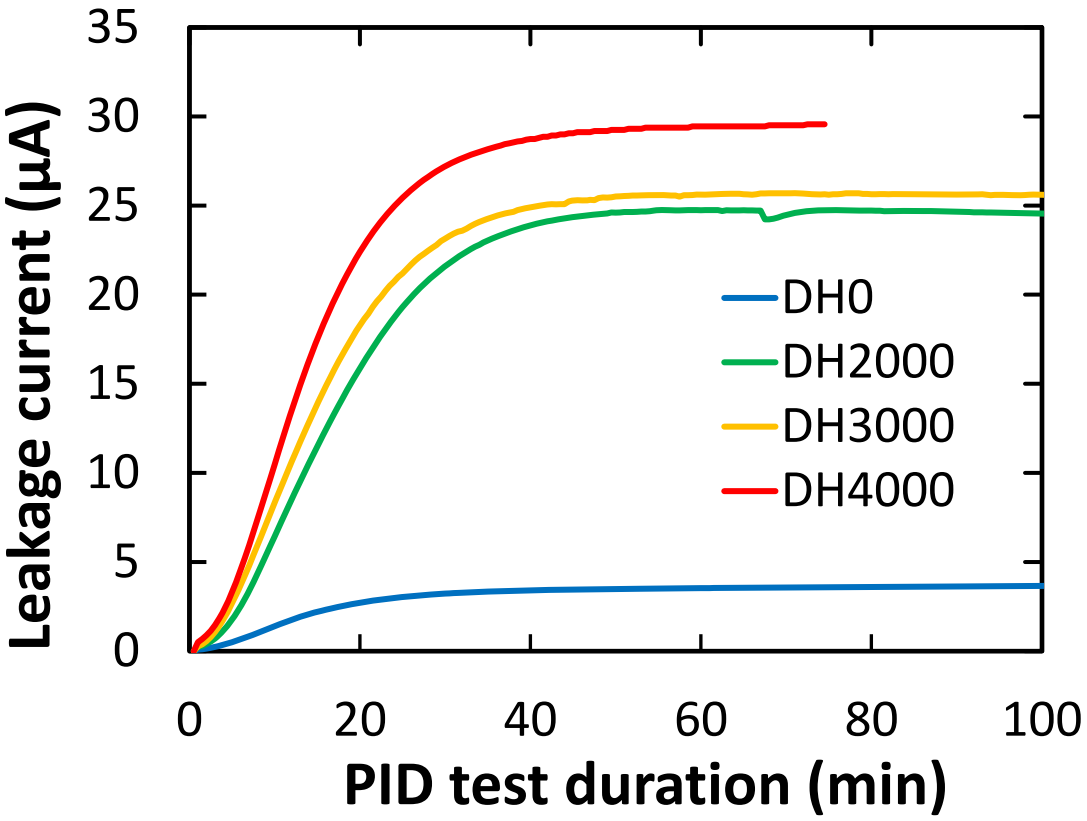

Fig. 4 (b). (Color online)

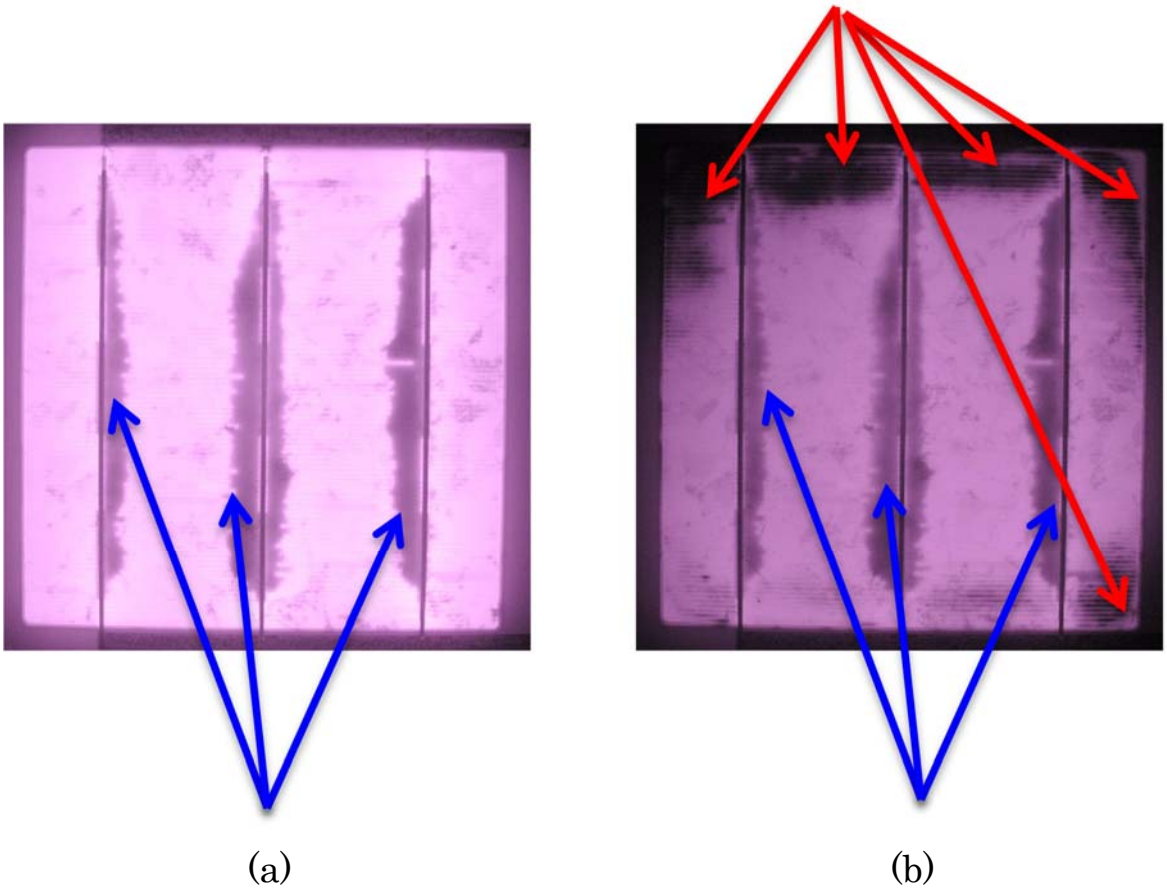

Fig. 5. (Color online)

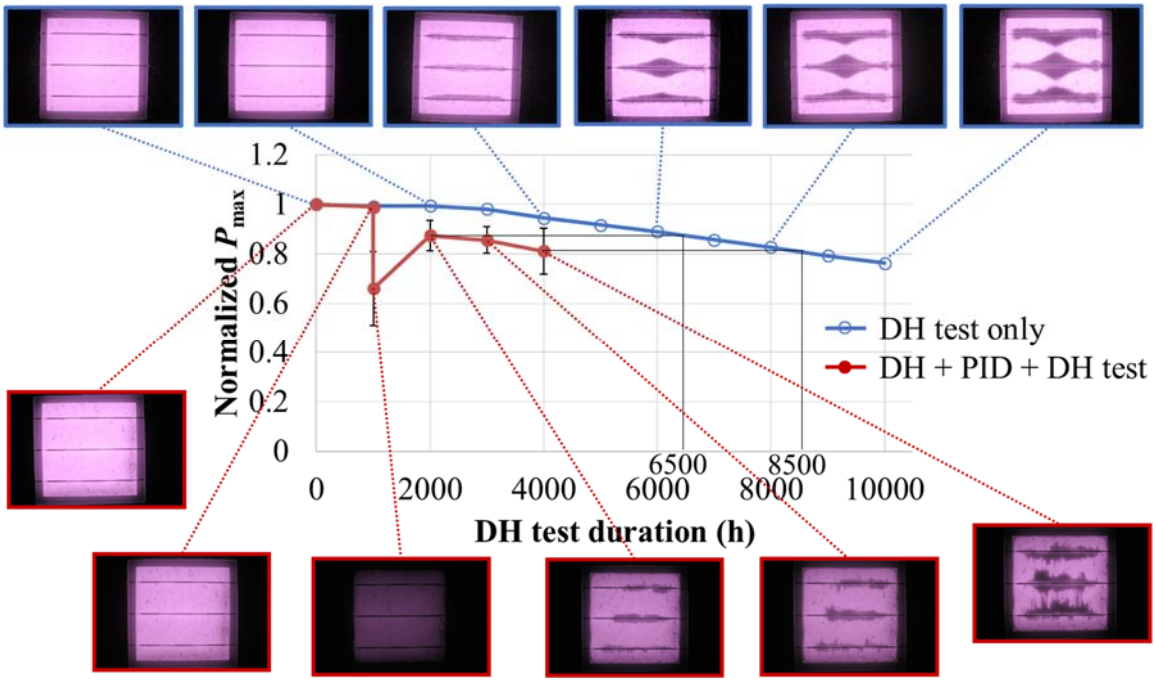

Fig. 6. (Color Online)

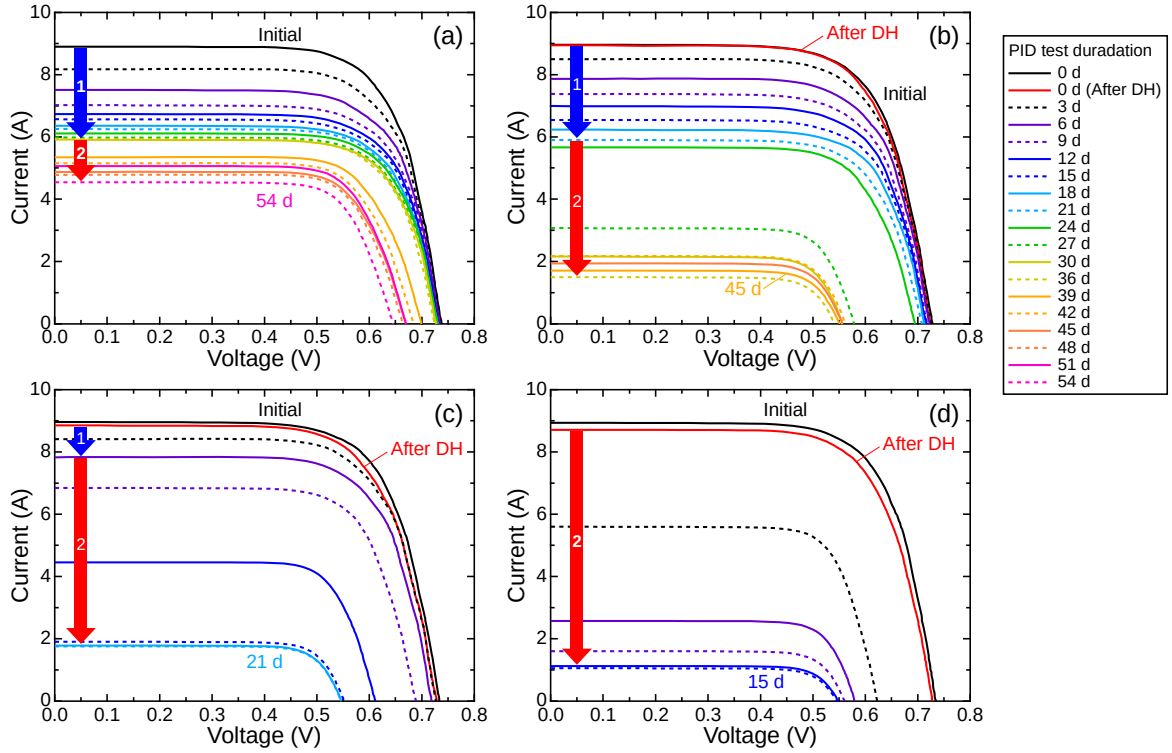

Fig. 7. (Color Online)

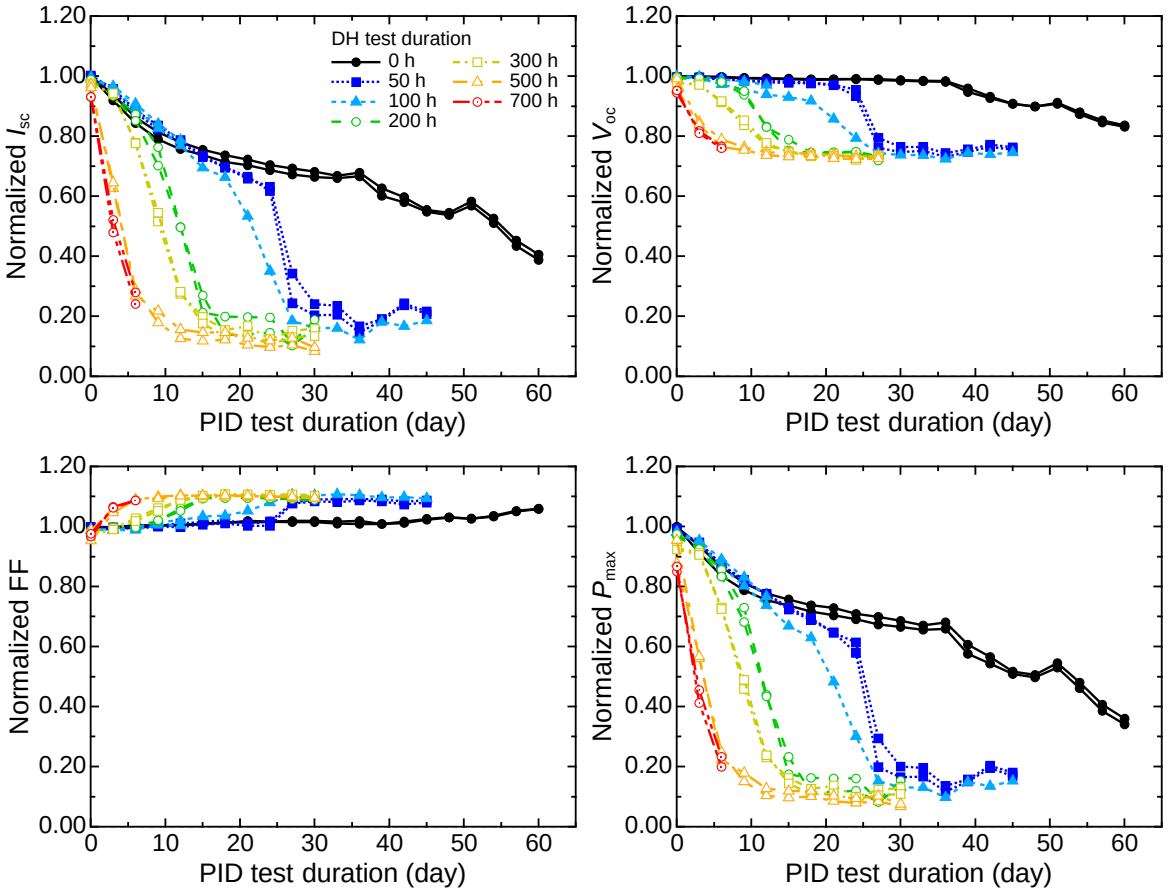

Fig. 8. (Color online)

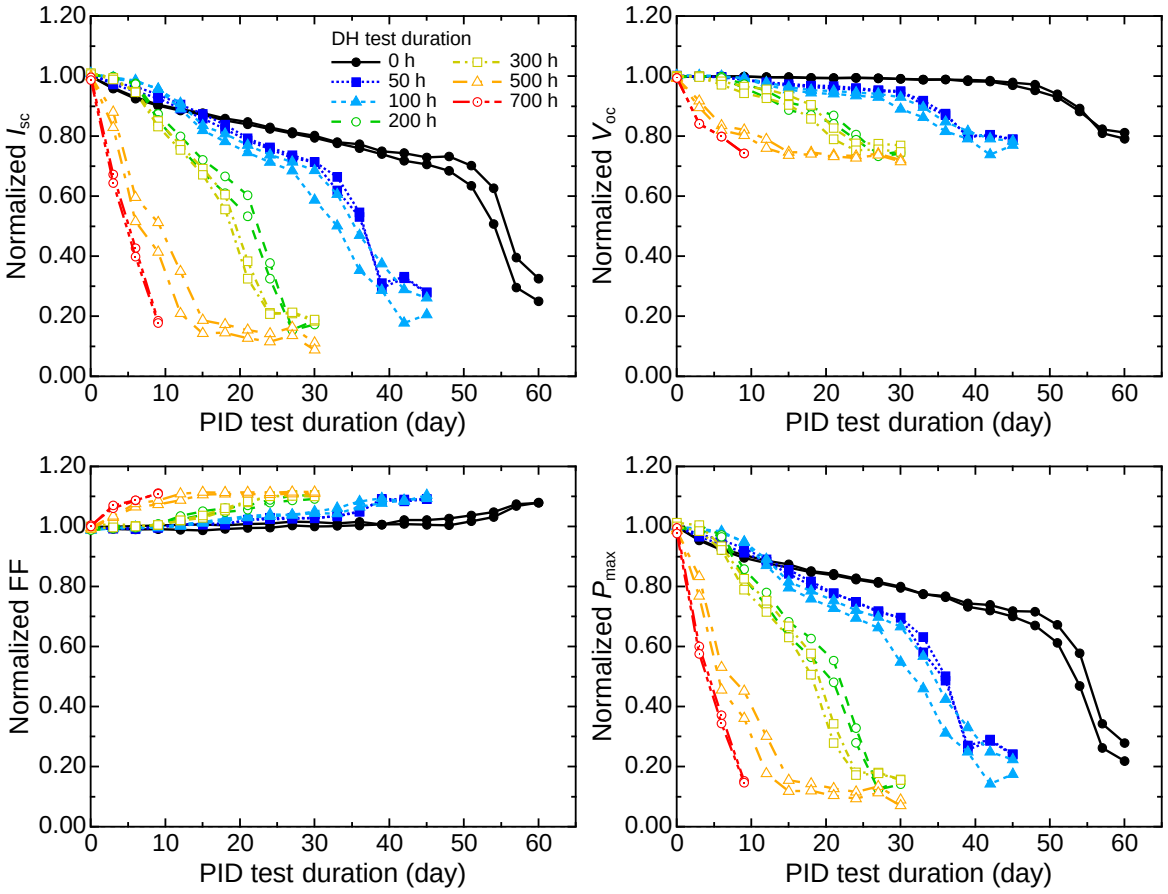

Fig. 9. (Color online)

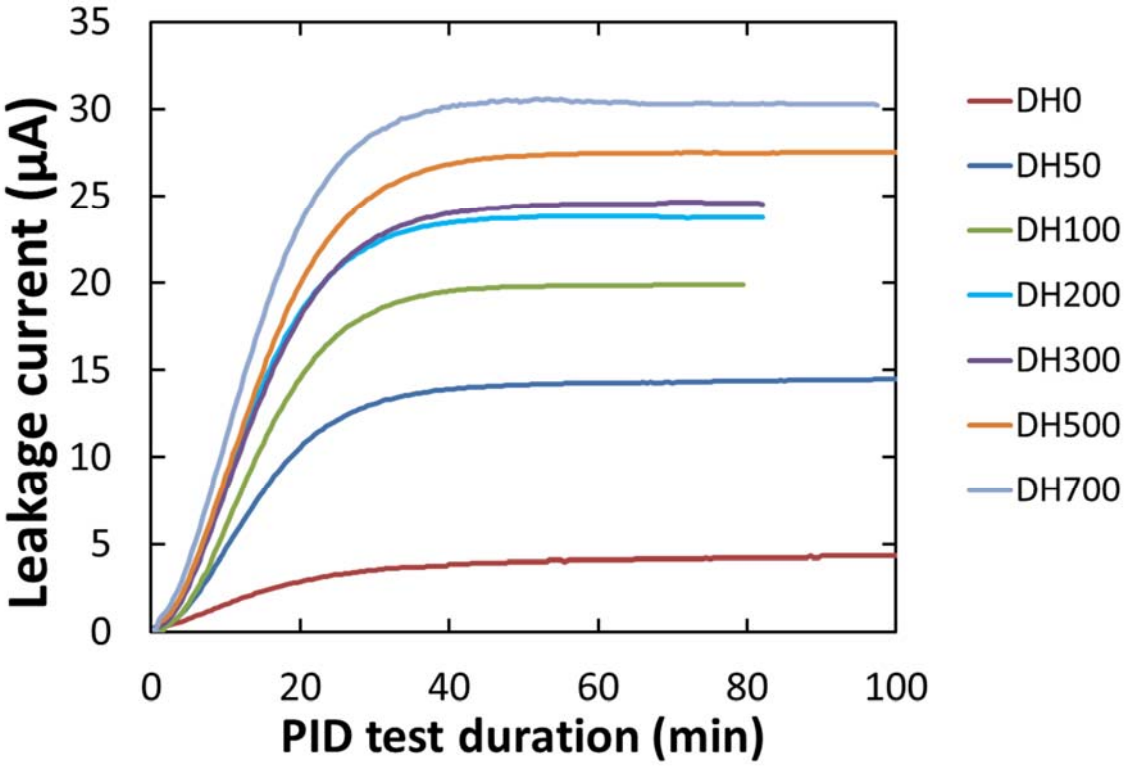

Fig. 10. (Color online)